Roto-translational states of the interstitial molecular hydrogen in silicon: A theoretical study

Vladlen V. Melnikov, and Sergei N. Yurchenko

Citation: J. Chem. Phys. **143**, 164305 (2015); doi: 10.1063/1.4934368
View online: https://doi.org/10.1063/1.4934368
View Table of Contents: http://aip.scitation.org/toc/jcp/143/16
Published by the American Institute of Physics

Roto-translational states of the interstitial molecular hydrogen in silicon: A theoretical study

Vladlen V. Melnikov[1,a] and Sergei N. Yurchenko[2]
[1]*Siberian Institute of Physics and Technology, Tomsk State University, Tomsk 634050, Russia*
[2]*Department of Physics and Astronomy, University College London, London WC1E 6BT, United Kingdom*

(Received 16 July 2015; accepted 11 October 2015; published online 23 October 2015)

A theoretical study of the interstitial molecular hydrogen in the silicon single-crystal is reported. H_2 and Si have been approximated as a rigid object and a static matrix, respectively. A five-dimensional numerical-analytical representation of an *ab initio* potential energy surface of the system has been constructed. This representation has been used to calculate rotational, translational, and roto-translational energy levels of the interstitial hydrogen, where three levels of theory, 2D, 3D, and 5D were considered. The potential energy surface, the band structure of energy levels, and the roto-translational states obtained are presented together with the symmetry analysis of the roto-translational wavefunctions. © *2015 AIP Publishing LLC*. [http://dx.doi.org/10.1063/1.4934368]

I. INTRODUCTION

Silicon is a widely applicable material in semiconductor device development and fabrication. Interstitial hydrogen is known to have significant influence over the physical and chemical properties of semiconductors.[1] Hydrogen penetrates into the structure of semiconductors at almost all technological stages, for example, during annealing, sintering, dry and wet etching, or cleaning by solvent processes. The presence of atomic hydrogen leads to the appearance of shallow and deep donor electron levels. Some of the hydrogen atoms that penetrated into the semiconductor crystalline structure form molecular hydrogen[2] which has practically no influence on the electrical and optical properties of the crystal and thus is difficult to detect. These hidden defects can be reactivated into their atomic form and thereby change the properties of the sample. For a number of technologies it is important to be able to control the diffusion and distribution of hydrogen inside a semiconductor. A detailed investigation of the hydrogen presence effects in silicon and other semiconductors is a challenging problem aimed to assist in related R&Ds.

The stability of molecular hydrogen in the crystalline silicon was first predicted more than 30 years ago by two independent groups.[3,4] However the detection of H_2 in semiconductors for many years remained unfeasible and was finally resolved with the help of Raman spectroscopy.[2] Results of dozen of experimental and theoretical studies on the properties of hydrogen in semiconductors have been reported (see, for example, Refs. 1–21 and references therein).

The stability, equilibrium positions, vibrational frequencies, and energy characteristics of H_2 in silicon were investigated *ab initio*.[5–10] Porter, Towler, and Needs[11] carried out the quantum-mechanical calculations of zero-point oscillations and energy levels hyperfine structure of hydrogen. A combined *ab initio* and classical molecular dynamics calculations were presented by Estreicher *et al.*[12] Fowler, Walters, and Stavola[13] studied rotational and vibrational properties of interstitial H_2 and its isotopologues in crystalline silicon by using a potential energy function represented as a superposition of potentials for two separated hydrogen atoms from Ref. 11. The experimental investigation by Markevich and Suezawa[14] deals with the O–H complex kinetics in the crystalline silicon. The *ortho-para* conversion of the interstitial H_2 in Si was studied in Refs. 15–19. A theoretical study of the rotational energy states of the hydrogen molecule in the silicon crystal within the framework of 2D quantum-mechanical model was presented in our recent work,[20] which was followed by a rather detailed investigation of the structural and energy properties of the H_2–Si system based on *ab initio* calculations.[21]

It should be mentioned that translation-rotation dynamics of H_2 and its isotopologues inside nanoscale cavities has been investigated rigorously and in great detail for the past decade by means of quantum 5D calculations. For instance, in Refs. 22–25 investigations of molecular hydrogen in clathrate hydrate cages were presented. Several works were devoted to the study of H_2 inside the fullerenes C_{60},[26–29] C_{70},[29] open-cage fullerene,[30] and in the interstitial sites of solid C_{60}.[31] These theoretical studies revealed a picture of intricate quantum dynamics, arising from the interplay between the symmetry of the confining nanospaces and the translation-rotation coupling.

As it follows from the above mentioned studies the hydrogen molecule interacts quite strongly with the silicon crystal which leads to a noticeable increase in the length of the H–H bond and a decrease in the vibrational frequencies. However along with this H_2 behaves as a nearly free rotator, i.e., the rotational degrees of freedom are not frozen and the existing spectra of the interstitial defect can be interpreted within the framework of a free molecule model. At the equilibrium configuration the H_2 center of mass is found at the tetrahedral position (T site) of the Si crystalline lattice and the molecule is oriented along the equivalent to the [100] crystallographic directions. The corresponding rotational potential barrier is

[a]Author to whom correspondence should be addressed. Electronic mail: melnikov@phys.tsu.ru

of the order of 0.01 eV. According to the experiment[14] the activation energy of the molecular hydrogen diffusion is 0.78 ± 0.05 eV.

In this work we present a theoretical study of energy states of the interstitial molecular hydrogen in the silicon single-crystal. *Ab initio* energies of the H_2–Si system calculated in Ref. 21 were used to construct a five-dimensional numerical-analytical representation of the potential energy surface (PES). This PES representation was used to calculate rotational, translational, and roto-translational energy levels of the interstitial hydrogen variationally. In order to take into account the periodicity of the H_2–Si interaction potential and estimate H_2 tunneling properties, the expected band structure of energy levels was calculated using a reduced 3D model approach.

II. THEORY

A theoretical treatment of the H_2–Si system is carried out in accordance with the adiabatic approximation. To study states of the interstitial molecular hydrogen in the silicon single-crystal we employ the following model. The molecule is considered as a rigid diatomic object with the bond length fixed at its average position. The crystal is substituted by a static matrix representing a periodic atomic structure. Thus in this model the system has five degrees of freedom (two rotational and three translational) and possess the appropriate T_d point group symmetry. The model is based on the facts that the proton is notably lighter than the silicon atom and H_2 is a rigid molecule and quite stable inside the crystal. In spite of the relative crudeness of this model we expect that it can provide a reasonable description of the system especially for low temperatures.

Our Hamiltonian of the H_2–Si system has the following form (see also Ref. 22):

$$\hat{H} = \frac{\hat{\mathbf{P}}^2}{2M} + \frac{\hat{\mathbf{J}}^2}{2\mu\rho^2} + V(\mathbf{R},\theta,\phi), \tag{1}$$

where $\hat{\mathbf{P}}$ is the center-of-mass momentum operator of the H_2 molecule with the total mass M, $\hat{\mathbf{J}}$ is the molecule angular momentum operator, ρ is the average H_2 bond length inside the crystal, μ is the molecule reduced mass. The function $V(\mathbf{R},\theta,\phi)$ is the corresponding potential energy, θ and ϕ are spherical coordinates defining the orientation of the molecule and $\mathbf{R} = (X,Y,Z)$ are the Cartesian coordinates of the molecule center of mass; the value $\theta = 0$ corresponds to the orientation of H_2 along the Z axis. It is assumed that the PES is known here. All necessary information concerning calculation and representation of the potential function is presented in Sec. III.

The corresponding stationary Schrödinger equation with the Hamiltonian in Eq. (1) and the periodic boundary conditions was solved numerically using the variational approach. The computational algorithm is realised as a FORTRAN program. The ansatz composed by the products of the plane waves and the spherical harmonics is defined by the following expansion:

$$\Psi_{\mathbf{k}n}(\mathbf{R},\theta,\phi) = \sum_{\mathbf{G},l,m} a_{lm}^{\mathbf{k}n}(\mathbf{G}) \exp[i(\mathbf{k}+\mathbf{G})\mathbf{R}]\, Y_l^m(\theta,\phi), \tag{2}$$

where $\mathbf{G}$ are reciprocal lattice vectors, $\mathbf{k}$ is a wavevector, $a_{lm}^{\mathbf{k}n}(\mathbf{G})$ are coefficients to be determined, and n is a serial number of the state. The summation over l and m is limited by $l_{\max}$ for the spherical harmonics Y_l^m and by the cutoff energy E_{cut} for the plane wave basis set, i.e., $l \leqslant l_{\max}$ and $|\mathbf{G}|^2/2 \leqslant E_{\text{cut}}$.

It should be noted that the plane wave basis set was chosen since it allows to consider the system both with periodic infinite and finite potentials. If the molecule is well localized in the vicinity of its equilibrium position, it can be treated isolated in a single box which corresponds to the calculations at the Γ point.

The crystal structure is defined by a unit cell with the lattice vectors **a**, **b**, and **c**, which in turn uniquely determine the periodic boundary conditions. To calculate the translational matrix elements of the Hamiltonian in Eq. (1) a uniformly distributed grid of $N_a \times N_b \times N_c$ points for the Cartesian coordinates $\mathbf{R}$ with the discretization steps $|\mathbf{a}|/N_a$, $|\mathbf{b}|/N_b$, and $|\mathbf{c}|/N_c$ for respective directions was used. Hereafter, the coordinates of an ith point will be denoted by $\mathbf{R}_i$.

The matrix elements of the Hamiltonian are calculated in two steps. At first their angular components are computed analytically. To this end the potential energy function is represented as an expansion in terms of the spherical harmonics at each grid point $\mathbf{R}_i$,

$$V(\mathbf{R}_i,\theta,\phi) = \sum_{l=0}^{6} \sum_{m=-l}^{l} g_{lm}(\mathbf{R}_i) Y_l^m(\theta,\phi). \tag{3}$$

The corresponding expansion parameters g_{lm} are determined on-the-fly through numerically precise fitting to the PES values by means of the least squares technique (see below for details about the PES). Subsequent step calculations are carried out using the discrete Fourier transform. When all of the matrix elements evaluated, the Hamilton matrix is diagonalized and the corresponding eigenvalues and eigenvectors are stored for further analysis.

III. POTENTIAL ENERGY SURFACE

A. *Ab initio* calculations

The adiabatic potential energy surface of the ground electronic state of the H_2–Si system has been calculated using the density functional theory with the PW91 exchange-correlation functional[32] in the generalized gradient approximation[33,34] as implemented in the CRYSTAL09 code.[35,36] Most of the *ab initio* calculations were carried out in Ref. 21 and the same data are employed in the current study. For the sake of completeness and consistency in the following the details of those calculations are reproduced.

The system was treated within the framework of the cubic supercell model with the periodic boundary conditions. The size of the cell was chosen so as to exclude the interaction of the hydrogen molecule with its periodic images. In these calculations supercells consisting of 4 and 32 primitive cells of crystalline silicon were used, containing 8 and 64 silicon atoms, respectively. The final PES calculations were carried out using the smaller cell. To check the quality of this model, the calculations for some selected atomic configurations were

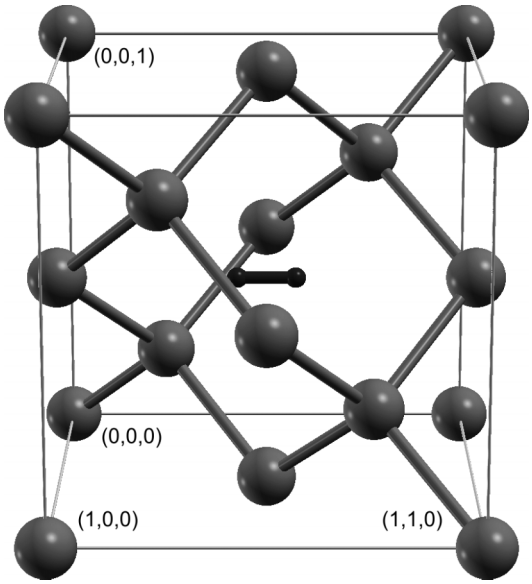

FIG. 1. The supercell used in the *ab initio* calculations consisting of eight Si atoms and one hydrogen molecule at the T site located exactly at the center of the cube. The Cartesian coordinates of four Si atoms in fractional units indicate the orientation of the XYZ reference frame.

repeated using the larger cell, which showed a small difference of the order of 10 cm^{-1}.

The small supercell is shown in Fig. 1. The Cartesian coordinate system is chosen such that its axis directions coincide with the supercell ones. Hereinafter, we mainly use this reference frame both in connection with angstrom and fractional units.

In the course of all calculations the Si atoms were fixed at their equilibrium positions of the corresponding crystal. *Ab initio* energies of the H_2–Si system were obtained for a large number of possible positions of H_2 inside the cell using a $8 \times 8 \times 8$ grid of k-points for the smaller cell and a $4 \times 4 \times 4$ grid for the larger one. Based on the preliminary calculations (such as reproduction of structural and energy properties) the optimized basis set by Torres *et al.*[37] for Si and the Dunning DZP basis set[38] for the hydrogen atoms were chosen. Due to the use of the Gaussian basis functions in our calculations the basis set superposition error (BSSE) correction was always taken into account.

The calculated bond length of the free H_2 molecule was found to be 0.7487 Å (slightly greater than the experimental value of 0.7414 Å, e.g., see Ref. 39) and 0.7810 Å for the hydrogen at the T site in the silicon crystal. The latter number was used in the *ab initio* calculations. It should be noted that our value of the silicon lattice parameter (a = 5.47 Å) differs from the experimental one (a = 5.43 Å) by not more than 0.7%. A potential barrier between two neighbouring T sites is found to be about 7961 cm^{-1} and of the same order of magnitude as the experimental value.[14] A calculated global minimum energy of the system relative to free H_2 and defect-free Si is about $1.1 \cdot 10^4$ cm^{-1} (1.4 eV). More detailed information about the *ab initio* PES properties, including the minimum energy path and preferable H_2 orientations in the crystal, can be found in Ref. 21.

B. Potential energy surface representation

We use the following analytical function to represent the *ab initio* potential energy surface of H_2 in the crystalline silicon:

$$V(\mathbf{R},\theta,\phi) = \sum_{i=1}^{N} \left[V_R(r_i) + V_\alpha(r_i,\alpha_i)\right], \tag{4}$$

where the summation runs over the surrounding Si atoms, r_i is the distance between the center of mass of H_2 and the ith Si atom, α_i is the angle between the hydrogen bond and a line connecting the center of mass and the corresponding Si atom. It is obvious that the distances r_i depend on the translation position vector $\mathbf{R}$ only, while the angles α_i depend both on $\mathbf{R}$ and θ,ϕ. The two-body radial V_R and angular V_α components of the pairwise potential are defined by the following expressions:

$$V_R(r) = \left[\frac{\epsilon_{12}}{r^{12}} + \frac{\epsilon_6}{r^6} + \frac{\epsilon_2}{r^2} + \frac{\epsilon_1}{r^1} + D_1 e^{-\beta r} + D_2 e^{-2\beta r} + \Delta_G(r)\right] \times f_\sigma(r), \tag{5}$$

$$V_\alpha(r,\alpha) = \left[G_2 \cos^2\alpha + G_4 \cos^4\alpha\right] \times f_\sigma(r). \tag{6}$$

For the very short distances between H_2 and Si ($r \leqslant r_{\min}$), the potential is set to a large value $V_{\max}$, which is also the largest value of the potential energy, i.e., a numerical substitution of the positive infinity, which otherwise would arise when two atoms approach each other. Only the Si atoms within the threshold radius $R_{\max}$ are taken into account to contribute to Eq. (4). Thus a finite number of atoms N is used to represent the crystal structure. The periodicity of the structure is taken into account at the programming level by reducing the translational coordinates $\mathbf{R}$ to the selected unit cell of the crystal.

The auxiliary function $f_\sigma(r)$ is responsible for the correct asymptotic of the two-body potential at large distances and defined as follows

$$f_\sigma(r) = \left[1 + \exp\left(\frac{r - r_{\max}}{\sigma}\right)\right]^{-1}. \tag{7}$$

An additional term $\Delta_G(r)$ in Eq. (5),

$$\Delta_G(r) = D_G \exp\left[-\beta_G (r - r_{\min})^2\right], \tag{8}$$

does not have physical meaning but allows to improve the form of $V_R(r)$ at small distances.

TABLE I. The potential energy surface parameters obtained by the fitting to the *ab initio* data.

Parameter	Value[a]
Fixed parameters	
$r_{\min}$	1.30
$R_{\max}$	8.00
σ	0.25
β_G	0.20×10^2
D_G	1.00×10^6
$V_{\max}$	1.00×10^{10}
Fitted parameters	
β	4.587 116 633 8
ϵ_1	$1.270\,263\,271\,8 \times 10^4$
ϵ_2	$-1.361\,267\,268\,9 \times 10^5$
ϵ_6	$8.528\,627\,857\,1 \times 10^6$
ϵ_{12}	$4.646\,997\,769\,3 \times 10^8$
G_2	$7.257\,764\,931\,0 \times 10^2$
G_4	$-2.223\,853\,034\,2 \times 10^3$
D_1	$-1.571\,968\,464\,5 \times 10^9$
D_2	$-2.627\,957\,732\,3 \times 10^{12}$

[a]Dimensions of the quantities correspond to the reciprocal centimeters for the energy and angstroms for the distance.

The parameters introduced in Eqs. (4)–(8) were determined by an iterative combination of fittings to the *ab initio* data and convergency analyses of the consequent variational calculations. The corresponding values are listed in Table I. The weighted standard deviation of the final fitting over 244 data points is 25.2 cm^{-1}, which is sufficiently accurate to maintain all important properties of the *ab initio* PES. Taking into account the level of the *ab initio* theory employed, fitting quality, complexity, and scale of the system under consideration we conclude that this representation is reasonably accurate to be used for calculations of energy states of the hydrogen molecule in the silicon crystal. Moreover our numerical-analytical PES possesses correct symmetry properties of the system and allows studying the interstitial defect properties both in the vicinity of the T site and in the whole bulk of the single-crystal.

Although most of the *ab initio* data points were selected around the equilibrium position, our representation reproduces other important regions also sufficiently well, including the minimum energy path. For instance, for the minimal/maximal values of the saddle point using Eqs. (4)–(8) we obtained 7769/9073 cm^{-1} which are comparable with the original *ab initio* values of 7961/8947 cm^{-1}. These two extreme values for the saddle point correspond to two different orientations of the molecule ($\theta_{\min} = 129.1°$, $\theta_{\max} = 54.7°$, $\phi_{\min} = \phi_{\max} = 45°$) with the same position of its center of mass in the (5/8, 5/8, 5/8) and equivalent points.

Contour plots of the PES up to 10 000 cm^{-1} in the XY plane for $Z = 0$ and $Z = 0.5$ bohr are shown in Fig. 2. The XYZ origin corresponds to the T site here, H_2 has a fixed orientation along the X axis. One can see that in the closest vicinity of the T site the potential is nearly centrally symmetric. For the coordinate range shown the longitudinal motion of H_2 is less rigid than the sideways one.

The dependence of the potential energy function on the orientation of a hydrogen molecule is demonstrated in Fig. 3. As it could be expected the rotational barrier increases with the displacement from the equilibrium position. One should notice that due to the indistinguishability of two hydrogen atoms the rotational energy surface at the T site has a cubic symmetry.

IV. ROTO-TRANSLATIONAL STATES

A. Computational details

In order to analyse the H_2–Si system at different active degrees of freedom as well as to accomplish an additional verification of our new PES, the following three cases were

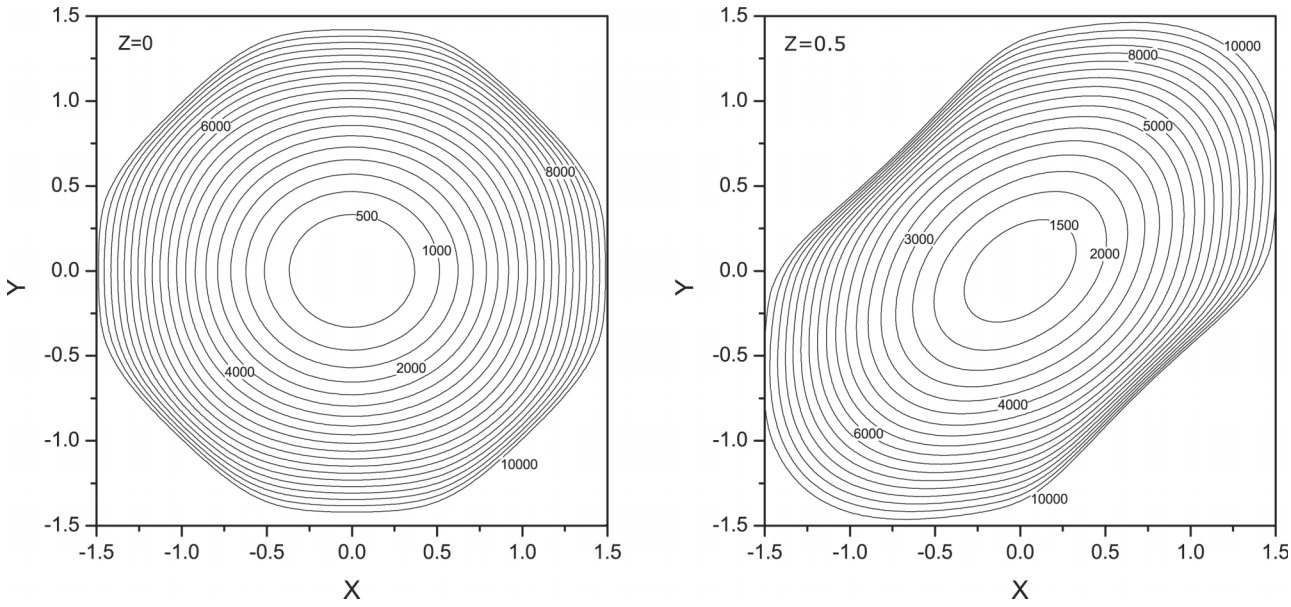

FIG. 2. The potential energy surface in the vicinity of the equilibrium position, plotted for fixed $Z = 0$ (on the left) and $Z = 0.5$ (on the right). The XYZ origin corresponds to the T site and the unit of length is bohr here. Isoenergetic contours are plotted at the step of 500 cm^{-1}. H_2 has fixed orientation along the X axis ($\theta = 90°$, $\phi = 0$).

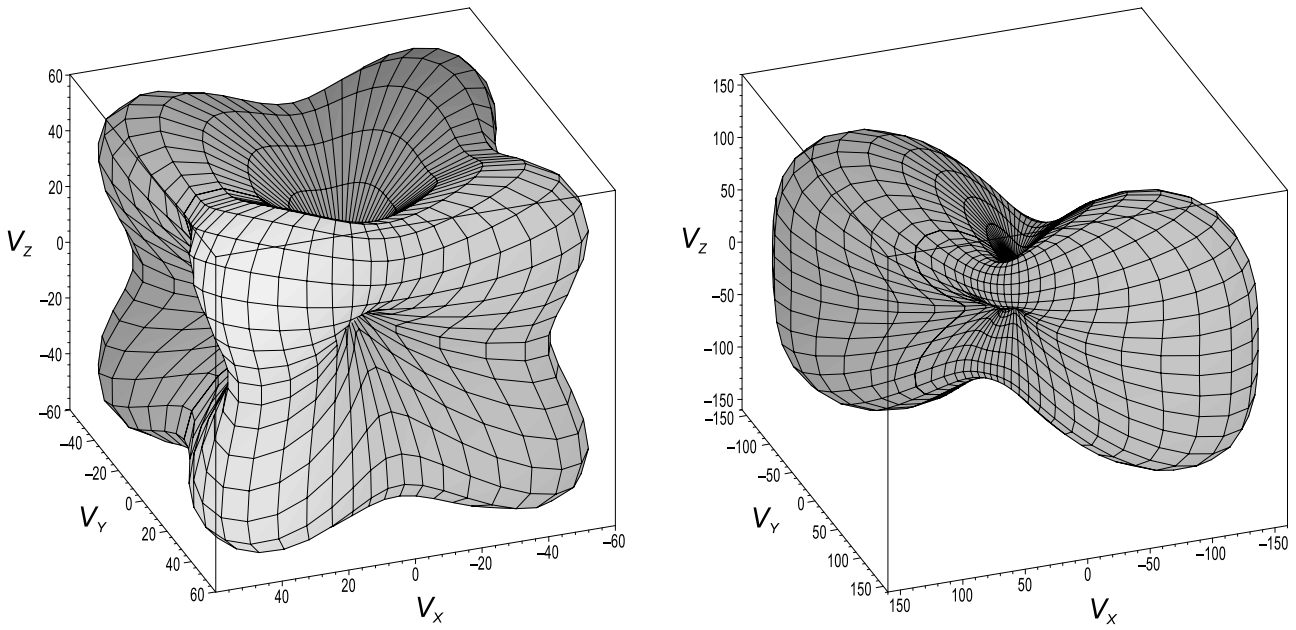

FIG. 3. The potential energy function (cm^{-1}) vs the orientation of the hydrogen molecule. The direction of a radius vector $\mathbf{V} = (V_X, V_Y, V_Z)$ at the point on the displayed surfaces is determined by the angles θ and ϕ, and its magnitude is equal to the values of the potential function V. The center-of-mass coordinates are fixed at $X = Y = 0$, $Z = 0$ (on the left) and $Z = 0.1$ bohr (on the right).

considered: rotational (2D), translation (3D), and roto-translation (5D) problems. The 2D rotational study was performed for the molecule center of mass fixed at the T site. To test the convergency we used $l_{\max}$ equals to 7, 10, and 15.

The 3D translation problem was realized by setting the rotational part in Eq. (2) to Y_0^0 only. This is analogous to the $J = 0$ state and *per se* equivalent to averaging of PES over the rotational variables at each **R** point. In the periodic description of the structure the primitive cell of the crystalline silicon was used. A uniformly distributed 3D grid contained $54 \times 54 \times 54$ points, the cutoff energy E_{cut} for the plane wave basis set was set to 16 000 cm^{-1}. In the low lying states (*quantum satis*) the H_2 molecule is mainly localized in the vicinity of the equilibrium position. Therefore, to span the whole space of the unit cell a rather large number of plane waves is required that makes the computations to be highly resource consuming and prevents a complete 5D calculations. The latter was done around the equilibrium region only.

The energy levels of the interstitial defect $E_{\mathbf{k}n}$ were calculated for the values of wavevector **k** that fall in the segments $L - \Gamma - X/X' - K - \Gamma$ connecting the high symmetry points of the Brillouin zone. Band formation was analyzed in the energy range up to 9000 cm^{-1} (hereinafter all energy values are given relative to the zero point energy). The present as well as previous[21] calculations reveal that there is no band formation taking place for energies below ~6000 cm^{-1}. Thus for the low-lying states the system can be considered at the Γ point only without any loss of physical information. Besides a localization of H_2 around the T site allows one to treat the system in a finite spatial domain at least for the states lying within this energy region.

To solve the 5D roto-translational problem we considered the system isolated in a cubic box with the T site located exactly at the center. To construct the box the PES was substituted by artificial infinite walls at the borders whereas inside the box the PES was represented by Eqs. (4)–(8). The dimension of the box a_{box} along with other parameters was selected by means of additional 2D and 3D calculations repeated with the presence of the box. In resultant computation $a_{\text{box}} = 0.4a$, $E_{\text{cut}} = 7000$ cm^{-1}, and the grid of $20 \times 20 \times 20$ points were used. The average H_2 bond length ρ was taken as $\hbar/\sqrt{2\mu B_0}$ with $B_0 = 52.683\,378$ cm^{-1} according to Ref. 20. To estimate the role of the translation - rotation interaction, the 5D results were compared to the calculations obtained by combining results of the 2D and 3D studies (2D+3D).

To assign the translational modes we use approximate quantum numbers (n_{h}, l_{h}) which correspond to the states of a three-dimensional isotropic harmonic oscillator. This choice is governed by the system symmetry as well as by the PES properties and reasonable at least for the low lying energy levels. To assign the rotational excitations we use an approximate quantum number J which corresponds to the largest contribution of the rotational basis functions Y_J^m to the wavefunction of the state. The contribution coefficients for the state n are calculated as follows:

$$C_J = \sqrt{\sum_{\mathbf{G},m} |a_{Jm}^{0n}(\mathbf{G})|^2}. \tag{9}$$

Thereby, the roto-translational energy state n is assigned (n_{h}, l_{h}) and J.

To analyse molecule localization behavior we calculate standard deviations of the center-of-mass coordinates ΔX, ΔY and ΔZ. For the n-fold degenerate states the wavefunctions related to the same energy are defined up to an arbitrary n-dimensional unitary transformation and to avoid ambiguity in this case the standard deviations were averaged over the corresponding degenerate states. As consistent with the system symmetry for the degenerate states $\overline{\Delta X} = \overline{\Delta Y} = \overline{\Delta Z}$ as well as for the nondegenerate states $\Delta X = \Delta Y = \Delta Z$.

Symmetry labeling of the states was accomplished according to the O_h point group for the rotational 2D calculations and the T_d point group for the translational 3D and roto-translational 5D calculations. In our group-theoretical analysis in the case of O_h point group the sets of spherical harmonics $\{Y_l^m\}$ belong to the following irreducible representations:[40] A_{1g} ($l = 0$), T_{1u} ($l = 1$), $E_g + T_{2g}$ ($l = 2$), $A_{2u} + T_{1u} + T_{2u}$ ($l = 3$), and $A_{1g} + E_g + T_{1g} + T_{2g}$ ($l = 4$). And in the case of T_d point group: A_1 ($l = 0$), T_2 ($l = 1$), $E + T_2$ ($l = 2$), $A_1 + T_1 + T_2$ ($l = 3$), and $A_1 + E + T_1 + T_2$ ($l = 4$). In order to label the calculated energy levels the symmetry properties of obtained wavefunctions were analysed. To determine the symmetry of the degenerate states the matrices of corresponding symmetry operations were generated and its traces were compared with the appropriate character tables.[40]

B. Results

The calculated low lying energy levels and some of their characteristics within the framework of different models are listed in Table II. Columns are labeled by the dimension of the problem in accordance with the computational details discussed above. The column labeled as $B_0J(J + 1)$ contains the rotational energies of the molecule in the rigid rotor approximation. All energy values are given relatively to the corresponding zero point energy.

TABLE II. Calculated energy levels of H_2 in silicon.

States		Properties (5D)		Energy levels (in cm^{-1})					
(n_h, l_h)[a]	J[b]	C_J[c]	ΔX[d]	5D calc.[e]	2D calc.[f]	3D calc.[g]	2D+3D calc.[h]	$B_0J(J+1)$	Exp.[16]
(0, 0)	0	0.987	0.21	0.00 (A_1)	0.00 (A_{1g})	0.00 (A_1)	0.00	0.00	
(0, 0)	1	0.995	0.21	103.45 (T_2)	105.20 (T_{1u})		105.20	105.37	99
(0, 0)	2	0.971	0.21	307.64 (T_2)	300.21 (E_g)		300.21	316.10	297
		0.997	0.21	310.37 (E)	327.06 (T_{2g})		327.06		
(0, 0)	3	0.870	0.23	588.59 (A_1)	622.79 (T_{1u})		622.79	632.20	
		0.949	0.22	610.32 (T_2)	635.97 (T_{2u})		635.97		
		0.932	0.22	612.15 (T_1)	652.97 (A_{2u})		652.97		
(1, 1)	0	0.956	0.26	727.38 (T_2)		715.27 (T_2)	715.27		
(1, 1)	1	0.992	0.27	802.87 (E)			820.47		
		0.929	0.26	847.07 (T_1)					
		0.942	0.26	853.71 (T_2)					
		0.865	0.25	853.80 (A_1)					
(1, 1)	2	0.792	0.25	930.83 (T_2)			1015.48		
		0.732	0.25	961.14 (A_1)			1042.33		
		0.766	0.25	961.69 (E)					
		0.757	0.25	967.85 (T_1)					
		0.983	0.27	1018.22 (T_2)					
		0.994	0.27	1027.72 (T_1)					
(0, 0)	4	0.770	0.23	1116.02 (A_1)	1040.51 (A_{1g})		1040.51	1053.67	
		0.795	0.23	1118.03 (E)	1047.08 (T_{1g})		1047.08		
		0.759	0.23	1126.21 (T_1)	1052.56 (E_g)		1052.56		
		0.812	0.23	1138.99 (T_2)	1067.32 (T_{2g})		1067.32		
(1, 1)	3	0.846	0.28	1257.70 (T_2)			1338.06		
		0.889	0.27	1273.80 (E)			1351.24		
		0.893	0.27	1301.48 (T_1)			1368.24		
		0.886	0.27	1301.67 (T_2)					
		0.922	0.28	1308.64 (A_1)					
		0.942	0.27	1325.59 (T_1)					
		0.951	0.27	1327.73 (T_2)					
		0.990	0.27	1341.99 (E)					
		0.997	0.27	1346.68 (A_2)					
(2, 0)	0	0.924	0.31	1442.22 (A_1)		1422.82 (A_1)	1422.82		
(2, 2)		0.928	0.31	1451.72 (T_2)		1426.51 (T_2)	1426.51		
		0.916	0.31	1466.82 (E)		1446.61 (E)	1446.61		

[a]The approximate quantum numbers corresponding to the states of a three-dimensional isotropic harmonic oscillator.
[b]The approximate quantum number corresponding to the rotational states of free molecule.
[c]The largest contribution of the rotational basis functions Y_l^m with $l = J$ to the corresponding wavefunction.
[d]The standard deviation of the X coordinate (in bohr). For the degenerate states the average values are presented.
[e]Roto-translational energy levels of H_2 at the Γ point. Symmetry labeling of the states (in brackets) is done according to the T_d point group.
[f]Rotational energy levels of H_2 calculated with the center of mass fixed at the T site. Symmetry labeling of the states is done according to the O_h point group.
[g]Translational energy levels of H_2 at the Γ point calculated with $l_{max} = 0$. Symmetry labeling of the states is done according to the T_d point group.
[h]The sum of the corresponding 2D and 3D values.

The degeneracy of the energy states calculated is in agreement with the system symmetry. Thus the 2D energy levels split exactly as predicted by the group theory[40] for the angular momentum in the cubic symmetry O_h. The splitting of the 3D energy levels is in line with the symmetry properties of the vibrational angular momentum in the T_d environment. Furthermore in spite of the translation-rotation interaction the symmetry of the 5D energy states correlates with the symmetry of the corresponding 3D and 2D states. For example, for the state ($n_h = 1$, $l_h = 1$, $J = 2$) we have $T_2 \times (E + T_2) = A_1 + E + 2T_1 + 2T_2$, etc.

One can see that the term values with $J \leqslant 2$ for the ground translational state (zero-point oscillations of the molecule as a whole about the T site, $n_h = 0$) are close to the experimental ones from Ref. 16 and comparable to the results obtained by Fowler, Walters, and Stavola.[13] These authors obtained 107.7 cm^{-1} and 89.1 cm^{-1} for the term $n_h = 0$, $J = 1$ without and with the zero-point motion taken into account, respectively. It should be noted that our calculations also show the tendency of lowering of the energy values when more degrees of freedom are included. However our values differ by less than 2 cm^{-1} (5D vs 2D calculations) in contrast to 18.6 cm^{-1} calculated using a more simple model.[13]

It should be noted here that the contribution coefficient C_J for the states with $J < 2$ is almost equal to unity. This fact is perfectly consistent with the nearly free rotator behaviour of an interstitial H_2 molecule.

It can be also seen that for $n_h = 0$, $J < 2$ the term values obtained for different models agree within about 2 cm^{-1} and due to the system symmetry they remain degenerate. The degeneracy is removed for the states with $J \geqslant 2$. Analyzing the magnitudes of the energy level splitting one can conclude that the translational - rotational interaction exercises a significant influence over the system properties and smoothes the effect of the rotational barrier for the low lying states. For example, for the states with $n_h = 0$, $J = 2$ a splitting of almost 27 cm^{-1} (2D) is reduced to the value of about 2.7 cm^{-1} (5D). It is reassuring that the results obtained with the most advanced level of theory considered in this work are in the best agreement with the experiment.[16]

Calculated standard deviations of the center-of-mass coordinate ΔX (for the degenerate states the averaged over the degenerate components) are also listed in Table II (5D problem). As it is expected the molecule is mainly localized in the vicinity of the equilibrium position and the root-mean-square amplitude grows with the increase of translational mode excitation. To show the localization domain the three-dimensional probability distribution functions were calculated as

$$P_{XYZ}(\mathbf{R}) = \int_0^{2\pi} d\phi \int_0^{\pi} d\theta \sin\theta \, |\Psi_{0n}(\mathbf{R}, \theta, \phi)|^2. \quad (10)$$

The plots of P_{XYZ} for the ground translation-rotation state and for the excited state ($n_h = 2$, $l_h = 0$, $J = 0$) are presented in Fig. 4. The ΔX values for these states are 0.21 and 0.31 bohr, respectively. Revealed dependencies are reasonable and very similar to the 3D isotropic harmonic oscillator ones.

We should also mention that the harmonic translational frequencies were found to be approximately 745 cm^{-1} and 727 cm^{-1} for the 3D and 5D models, respectively (estimated as two thirds of the corresponding zero point energies).

Visualization of the 3D translation solution is presented in Figs. 5 and 6. In accordance with the system symmetry the low lying energy levels are degenerate. An additional twofold degeneracy at fixed values of $\mathbf{k}$ arises due to the existence of two equivalent T sites in the primitive unit cell of silicon. When the energy increases, the probability of the molecule tunneling between the T sites grows and a band structure formation takes place. Moreover, in this case the magnitude of the energy level splitting Δ obtained at the Γ point corresponds to the width of the allowed band formed.

In Fig. 5 the values of the width Δ of the broadest allowed energy bands and energy levels $E_{\mathbf{k}n}$ ($\mathbf{k} = 0$) in the range from 6000 to 8500 cm^{-1} are shown. A weak splitting is observed for the energies of about 6170 cm^{-1} resulting in the band formation with $\Delta \approx 0.1$ cm^{-1}. This energy is by ~170 cm^{-1} higher than the corresponding value obtained in Ref. 21. For

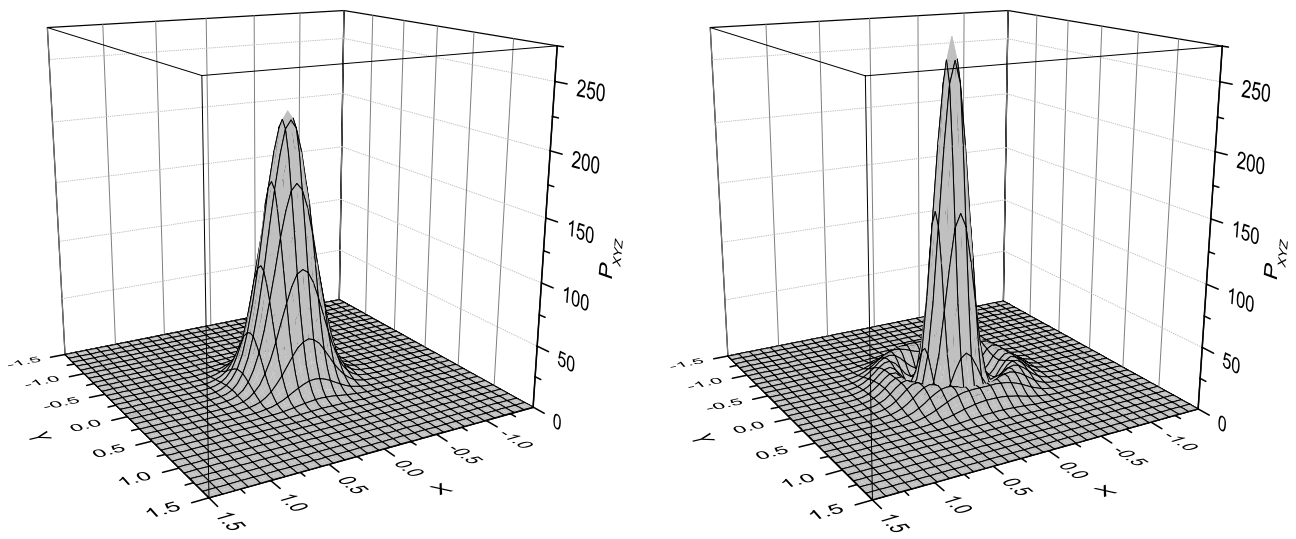

FIG. 4. The three-dimensional probability distributions functions for the ground translation-rotation state (on the left) and for the excited state ($n_h = 2$, $l_h = 0$, $J = 0$) (on the right). The XYZ origin corresponds to the T site and the unit of length is bohr here.

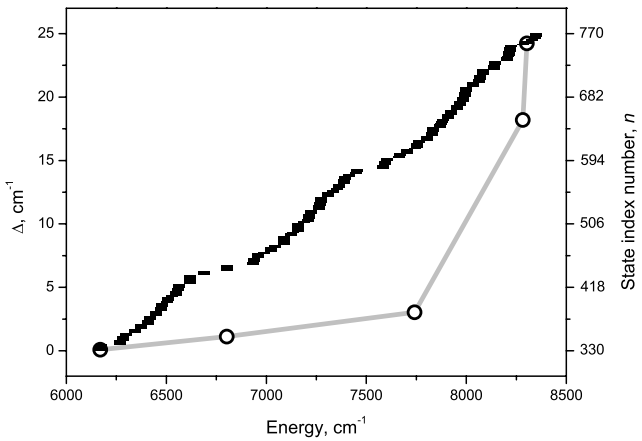

FIG. 5. The width values of the broadest allowed bands (circles) and the energy levels $E_{\mathbf{k}n}$ (dashes) for the energy region selected. The circles point out on the band bottom (abscissa value) and Δ corresponds to the band width. The energy level values $E_{\mathbf{k}n}$ vs its index number n at the Γ point are shown.

higher energies the band width increases, for instance, the allowed energy band with the width of approximately 1.1 cm^{-1} is close to 6803 cm^{-1}, while Δ exceeds 24 cm^{-1} already at 8304 cm^{-1}.

In Fig. 6 the band structure of energy levels in the range from 6802 to 6806 cm^{-1} is presented. Two allowed bands with Δ of about 1 cm^{-1} are found to be formed in this energy region. It should be noted that the dispersion laws in the segments $L-\Gamma-X/X'-K-\Gamma$ obtained in this work and in Ref. 21 do qualitatively agree with each other. Our calculations reveal quite similar dependencies but only at higher energy values. Thus an analogous band structure was obtained in Ref. 21 for the energy range lower by ~200 cm^{-1}.

Analysis of the corresponding group velocity of the molecule shows that this quantity is maximal for the [100] direction and minimal for [111]. This result is concordant with the observation of the hydrogen-containing planar defects (*platelets*) formed mainly in the {111} planes.[1] Despite the vacancy mechanism is considered to play a key role in the *platelets* formation, this orientation remains predominant even in terms of the ideal crystal model.

Another peculiarity of the calculated energy spectrum should be noted. For the energy range up to 9000 cm^{-1} there

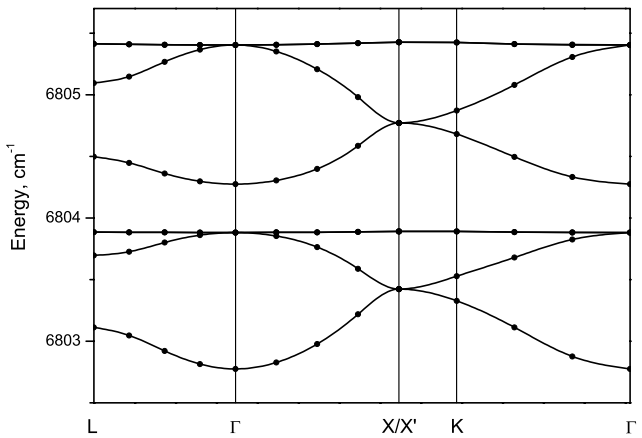

FIG. 6. The band structure of energy levels of H_2 in silicon.

are only a few allowed energy bands with $\Delta > 0.1$ cm^{-1} formed and most of the states are discrete. Two possible explanations can be suggested for this result. First, the region of the transition point between two neighbouring T sites is a bottleneck, i.e., the PES is quite steep there when the molecule moves away from the minimum energy path and thus the transition motion is hindered. Second, when H_2 passes from one T site to the nearest one, the orientation of H_2 relatively to the surrounding Si atoms changes (equivalent to a 90° rotation about one of X, Y, or Z axis). Therefore, one can suppose that only states with certain symmetries are involved in the band structure formation. As a result such restrictions can make additional contributions to the molecule T site confinement.

V. SUMMARY AND CONCLUSION

A theoretical study of H_2 in the silicon crystal was carried out. A five-dimensional numerical-analytical representation of an *ab initio* potential energy surface of the system was constructed, which preserves the main properties of the PES, including the correct geometry and symmetry.

The PES representation was used to calculate the rotational, translational, and roto-translational energy levels of the interstitial hydrogen. Three models were considered, 2D, 3D, and 5D. The results obtained with the most advanced level of theory (5D) are in the best agreement with the experiment. One can see that for $n_h = 0$, $J < 2$ the term values obtained for different models agree within about 2 cm^{-1} and due to the system symmetry they remain degenerate. Our calculations revealed that the translation - rotation interaction has a significant influence over the system properties and smoothes the effect of the rotational barrier for the low lying states.

Taking into account that H_2 is located in a periodic potential we calculated a band structure of energy levels using a reduced 3D model approach. For energies up to 9000 cm^{-1} there is not many allowed energy bands formed where most of the states are discrete. Nevertheless, an allowed energy band with the width about 1.1 cm^{-1} is close to 6803 cm^{-1}. The width of the band formed in the vicinity of 8304 cm^{-1} exceeds 24 cm^{-1}. The band structure properties analyzed agree with the observation of the *platelets* which are mainly formed in the {111} crystallographic planes.[1] Despite the vacancy mechanism is considered to play a key role, this orientation remains predominant even in terms of the ideal crystal model.

ACKNOWLEDGMENTS

Support from the Ministry of Education and Science of the Russian Federation (Objective No. 2014/223, Project Code No. 727) is acknowledged. The numerical calculations were performed on the SKIF-Cyberia supercomputer with the support of the Regional Center for Collective Use of High-Performance Computing Resources of Tomsk State University.

[1]S. J. Pearton, J. W. Corbett, and M. Stavola, *Hydrogen in Crystalline Semiconductors* (Springer-Verlag, Berlin, 1992).
[2]A. W. R. Leitch, V. Alex, and J. Weber, Phys. Rev. Lett. **81**, 421 (1998).
[3]A. Mainwood and A. M. Stoneham, Physica B **116**, 101 (1983).
[4]J. W. Corbett, S. N. Sahu, T. S. Shi, and L. C. Snyder, Phys. Lett. A **93**, 303 (1983).

[5]Y. Okamoto, M. Saito, and A. Oshiyama, Phys. Rev. B **56**, 10016 (1997).
[6]K. G. Nakamura, K. Ishioka, M. Kitajima *et al.*, Appl. Surf. Sci. **130**, 243 (1998).
[7]C. G. Van de Walle, Phys. Rev. Lett. **80**, 2177 (1998).
[8]C. G. Van de Walle and J. P. Goss, Mater. Sci. Eng., B **58**, 17 (1999).
[9]B. Hourahine, R. Jones, S. Oberg *et al.*, Phys. Rev. B **57**, 12666 (1998).
[10]Y.-S. Kim, Y.-G. Jin, J.-W. Jeong, and K. J. Chang, Physica B **273–274**, 231 (1999).
[11]A. R. Porter, M. D. Towler, and R. J. Needs, Phys. Rev. B **60**, 13534 (1999).
[12]S. K. Estreicher, J. L. McAfee, P. A. Fedders *et al.*, Physica B **308**, 202 (2001).
[13]W. B. Fowler, P. Walters, and M. Stavola, Phys. Rev. B **66**, 075216 (2002).
[14]V. P. Markevich and M. Suezawa, J. Appl. Phys. **83**, 2988 (1998).
[15]E. V. Lavrov and J. Weber, Phys. Rev. Lett. **89**, 215501 (2002).
[16]M. Hiller, E. V. Lavrov, and J. Weber, Phys. Rev. B **74**, 235214 (2006).
[17]M. Hiller, E. V. Lavrov, and J. Weber, Phys. Rev. Lett. **98**, 055504 (2007).
[18]J. Weber, M. Hiller, and E. V. Lavrov, Physica B **401-402**, 91 (2007).
[19]C. Peng, M. Stavola, W. B. Fowler, and M. Lockwood, Phys. Rev. B **80**, 125207 (2009).
[20]V. V. Melnikov and S. N. Yurchenko, Russ. Phys. J. **56**, 1363 (2014).
[21]V. V. Melnikov, J. Exp. Theor. Phys. **120**, 1005 (2015).
[22]M. Xu, Y. S. Elmatad, F. Sebastianelli, J. W. Moskowitz, and Z. Bačić, J. Phys. Chem. B **110**, 24806 (2006).
[23]M. Xu, F. Sebastianelli, and Z. Bačić, J. Chem. Phys. **128**, 244715 (2008).
[24]M. Xu, F. Sebastianelli, and Z. Bačić, J. Phys. Chem. A **113**, 7601 (2009).
[25]M. Xu, L. Ulivi, M. Celli, D. Colognesi, and Z. Bačić, Phys. Rev. B **83**, 241403(R) (2011).
[26]M. Xu, F. Sebastianelli, and Z. Bačić, J. Chem. Phys. **128**, 011101 (2008).
[27]M. Xu, F. Sebastianelli, Z. Bačić, R. Lawler, and N. J. Turro, J. Chem. Phys. **129**, 064313 (2008).
[28]M. Xu, M. Jiménez-Ruiz, M. R. Johnson, S. Rols, S. Ye, M. Carravetta, M. S. Denning, X. Lei, Z. Bačić, and A. J. Horsewill, Phys. Rev. Lett. **113**, 123001 (2014).
[29]M. Xu, F. Sebastianelli, B. R. Gibbons, Z. Bačić, R. Lawler, and N. J. Turro, J. Chem. Phys. **130**, 224306 (2009).
[30]S. Ye, M. Xu, Z. Bačić, R. Lawler, and N. J. Turro, J. Phys. Chem. A **114**, 9936 (2010).
[31]S. Ye, M. Xu, S. FitzGerald, K. Tchernyshyov, and Z. Bačić, J. Chem. Phys. **138**, 244707 (2013).
[32]J. P. Perdew, J. A. Chevary, S. H. Vosko *et al.*, Phys. Rev. B **46**, 6671 (1992).
[33]J. P. Perdew and Y. Wang, Phys. Rev. B **33**, 8800 (1986).
[34]J. P. Perdew, Phys. Rev. B **33**, 8822 (1986).
[35]R. Dovesi, R. Orlando, B. Civalleri, C. Roetti, V. R. Saunders, and C. M. Zicovich-Wilson, Z. Kristallogr. **220**, 571 (2005).
[36]R. Dovesi, V. R. Saunders, C. Roetti, R. Orlando, C. M. Zicovich-Wilson, F. Pascale, B. Civalleri, K. Doll, N. M. Harrison, I. J. Bush, P. DArco, and M. Llunell, *CRYSTAL09 User's Manual* (University of Torino, Torino, 2009).
[37]F. J. Torres, B. Civalleri, C. Pisani, and P. Ugliengo, J. Phys. Chem. B **110**, 10467 (2006).
[38]T. H. Dunning, Jr., J. Chem. Phys. **53**, 2823 (1970).
[39]I. S. Grigoriev, E. Z. Meilikhov, and A. A. Radzig, *Handbook of Physical Quantities* (CRC Press, Boca Raton, Florida, USA, 1996).
[40]F. A. Cotton, *Chemical Applications of Group Theory*, 3rd ed. (Wiley-Interscience, New York, 1990).